Structure Improvement and Joint Resistance Estimation in Demountable Butt and Edge Joints of a Stacked REBCO Conductor Within a Metal Jacket

Satoshi Ito, Tatsuya Ohinata, Leslie Bromberg, and Hidetoshi Hashizume

***Abstract*—Electrical (mechanical) butt and edge joints of a stacked REBCO conductor within a metal jacket have been investigated as candidates for demountable (remountable) electrical joints within demountable high-temperature superconducting magnets. This paper summarizes recent progress in the R&D of the two electrical joints. First, we have described recent R&D for the butt joint. We have previously established fabrication methods for the butt joint samples. In this paper, we have tried to establish a predictive method of joint resistance for a large-scale stacked REBCO conductor within a metal jacket by using small-scale experiments and current distribution analyses. For this purpose, we evaluated joint resistivity, particularly in the butt joint where an indium film is inserted between joint surfaces. Based on the small-scale experiments and 3-D current distribution analyses, the joint resistivity between the contact surface and the indium film inserted into the joint section is evaluated to be 1.1×10^{-12} Ωm^2. According to the discussion based on the results, the joint resistance for a 100-kA-class REBCO conductor is estimated to be 3.7 nΩ, which is a reasonably acceptable value from the viewpoint of electric power for cooling. Second, we recapitulate present R&D for the edge joint. In the case of the edge joint, adequate methods for fabricating samples had not been established because this joint has only been recently proposed. In a previous study, the experimentally measured joint resistance of the edge joint was much higher than predicted. We expect that the reason for the discrepancy is degradation of the conductor edge during the fabrication process and strains due to forces during the joint test. In addition, poor fabrication of the joint faces resulted in limited local area contact across the joint. In this paper, we improved the methods of fabrication and the structure of the test conductors based on numerical analysis. We then carried out a testing program of the edge joint of a stacked GdBCO conductor within a copper jacket fabricated with the improved process. The experimentally evaluated joint resistance agreed with numerical predictions. Therefore, the satisfactory performance of the edge joint was demonstrated in this paper.**

***Index Terms*—Fusion reactors, high-temperature superconductors, power cable connecting, superconducting magnets.**

Manuscript received October 9, 2012; accepted January 27, 2013. Date of publication February 1, 2013; date of current version May 15, 2013. This work was supported by the Ministry of Education, Culture, Sports, Science and Technology in Japan through Grant-in-Aid for Scientific Research (A), 23246159, 2012 and through Grant-in-Aid for Young Scientists (A), 23686132, 2012.

S. Ito, T. Ohinata, and H. Hashizume are with the Department of Quantum Science and Energy Engineering, Graduate School of Engineering, Tohoku University, Sendai 980-8579, Japan (e-mail: satoshi.ito@qse.tohoku.ac.jp).

L. Bromberg is with the Plasma Science and Fusion Center, Massachusetts Institute of Technology, Cambridge, MA 02139 USA (e-mail: brom@psfc.mit.edu).

Color versions of one or more of the figures in this paper are available online at http://ieeexplore.ieee.org.

Digital Object Identifier 10.1109/TASC.2013.2244197

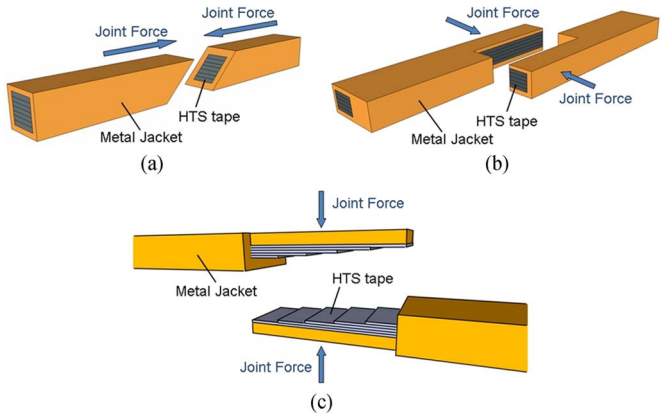

Fig. 1. Schematics of the electrical joints of stacked HTS conductors. (a) Butt joint. (b) Edge joint. (c) Lap joint.

I. Introduction

A demountable (remountable) high-temperature superconducting (HTS) magnet has been proposed for a small tokamak plasma-facing component test machine [1]–[4] and a heliotron-type fusion reactor [5]–[8]. The magnet consists of some segments that can be mounted and demounted repeatedly. The advantages of remountability are to simplify fabrication of large and complex superconducting magnets, to repair failed segments, and to obtain good access to inner reactor components. An HTS material is used in the magnet. The HTS materials are robust against heat generation because of their high critical current and heat capacity at relatively high operating temperature ($>$ 20 K). This fact allows demountable electrical (mechanical) joints, which are resistive. The joint resistance can be higher than with low-temperature superconducting (LTS) because refrigeration power decreases with higher operating temperatures.

Among currently developed HTS tapes or wires, REBCO tapes (called 2G HTS tapes or coated conductors) are attractive candidates for a demountable magnet because they can keep their critical current at high field at a relatively high operating temperature. Fig. 1 illustrates electrical joints of stacked REBCO conductors, which have been investigated in previous studies: 1) electrical butt joint [8], 2) electrical edge joint [4], and 3) electrical lap joint [9]–[11]. In the case of the lap joint, gap and misalignment at the joint section can cause an increase in joint resistance and inserting a compliant metal layer such as indium film is needed to solve the problem [10]. When indium

films are used in the lap joints, constituted layers of the REBCO tape detach as segments of the magnet are demounted. On the other hand, the other two joints can prevent the layers of a REBCO tape from detaching when the magnet is demounted, although an indium film is inserted between joint surfaces to reduce joint resistance. The lap joint with an indium film can be used for a segmented HTS magnet [11], [12], constructed by connecting short conductors with a permanent (nondetachable) joint method; HTS tapes are connected with the lap joint, and jackets are welded. Alternatively, the lap joint could be used for the demountable magnet if the compliant metal film is not indium but rather annealed copper. As aforementioned, the butt and edge joints with any compliant metal layers can be demountable.

This paper summarizes recent research activities on the demountable butt and edge joints. In Section II, we describe experimental and numerical estimations of joint resistance in the butt joint of a stacked REBCO conductor within a copper jacket. In previous studies [6]–[8], we have already established methods for fabricating samples for the butt joint. In the present phase, we have tried to estimate the joint resistance of a large-scale stacked REBCO conductor by using small-scale experiments and current distribution analyses. In a previous study [8], we evaluated the joint resistance in the butt joint based on 2-D current distribution analyses and an experiment using stacked GdBCO conductors within a copper jacket. The study showed that the joint resistance can be reduced by increasing the joint area of the conductive metal layers (thickness of the metal layers) in the REBCO tape, such as silver and copper layers. However, the experimental result did not show good agreement with the numerical prediction due to the existence of a current pathway through the jacket, which was not considered in the numerical analysis. In this paper, therefore, we carried out joint tests and 3-D current distribution analyses to evaluate the contact resistivity, which is needed to predict the joint resistance of a REBCO conductor having large current capacity, for example, 100 kA for a heliotron-type fusion DEMO reactor, FFHR [11], [12]. In the joint test, we used the conductor having a low-electrical-conductivity material inserted between the stacked tapes and the jacket. The conductor structure can largely prevent current from flowing through the jacket in the joint region. Furthermore, we measured the joint resistance for various configurations of contact surface. In the current distribution analyses, the joint resistance was evaluated with a 3-D numerical model that simulates the butt joint of the conductor, including the copper jacket. Based on the results, the contact resistivities in the configurations were evaluated. Finally, the total joint resistance and electric power for cooling the magnet (for FFHR, as an example) were estimated by the distribution analyses with the evaluated contact resistivity.

In Section III, we describe improvements to the joint structure and the fabrication process of samples for the edge joint. In the edge joint, the side edges of a stacked HTS conductor embedded in a metal jacket are mechanically jointed. The electrical edge joint has some advantages compared with the butt joint and the lap joint, e.g., a larger joint area can be easily obtained, a sliding motion of the joint surfaces can be tolerated, and fabrication of the joint section in a demountable magnet can be relatively easy. However, we had not been able to establish a method for fabricating samples for the edge joint that has low joint resistance. In a previous study [4], we numerically estimated the joint resistance of the edge joint of a stacked REBCO conductor and concluded that the edge joint should have better performance than the electrical lap joint, in the case of large-scale conductors. We also tried to fabricate a sample (40-layered stacked YBCO conductor within a copper jacket) for the edge joint. In the edge joint, the side face of the jacket has to be removed to make the joint surface. For this purpose, we milled the side face of the jacket and the YBCO tapes. However, the experimentally measured joint resistance in the edge joint turned out to be much higher than predicted. We speculated that the reason for the discrepancy was degradation of the conductor edge during the fabrication process and strains due to forces during the joint test. In addition, poor fabrication of the joint faces resulted in limited local area contact across the joint. In this paper, we improved the fabrication methods to assure parallel surfaces across the joint and to avoid the degradation due to the force and the fabrication. We also predicted the joint resistance in the edge joint of the improved conductor by 2-D numerical analysis. We then tested the edge joint of a stacked GdBCO conductor within a copper jacket fabricated with the improved process. We compared the experimental measurements of the joint resistance with numerical calculations.

Finally, we draw conclusions from the obtained results on the two demountable joints of a stacked REBCO conductor within a metal jacket in Section IV.

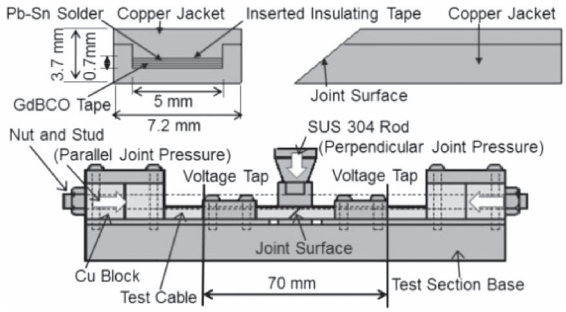

Fig. 2. Test conductor and section in the butt joint.

II. Joint Resistance Estimation in the Butt Joint

A. Experimental Evaluation

In this section, we describe our experimental procedure and results of the butt joint test. Fig. 2 shows a test conductor and a test section. Stacked GdBCO conductors within a copper jacket were used for the joint test. The conductor was made by stacking four GdBCO tapes and one stainless steel tape (5-mm wide) inside the copper jacket. They were fixed with Sn63Pb37 solder. The stainless steel tape was on the top of the stacked four GdBCO tapes. A polyimide tape was placed on top of the stainless steel tape for insulating the stacked tapes from the copper jacket. The GdBCO tape (FYSC-SC05, Fujikura Ltd.) has a layer structure of Hastelloy substrate (100 μm)/buffer layers (0.5 μm)/GdBCO (1.5 μm)/silver (20 μm)/solder

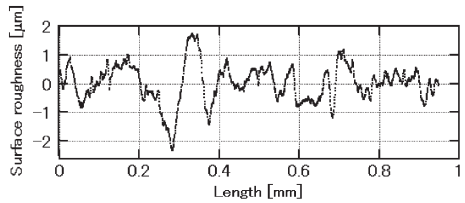

Fig. 3. Profile of the joint surface.

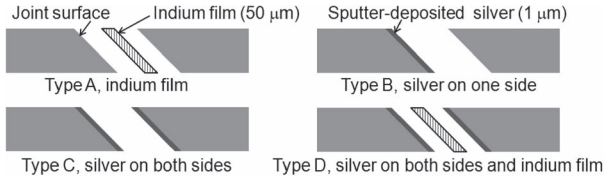

Fig. 4. Contact surface configurations.

(2–4 μm)/copper (100 μm). The critical current of the tapes used for the samples is 260 A at 77 K, self-field. After fabricating the stacked GdBCO conductor, we measured a critical current of the test conductor of 760 A at 77 K, self-field (1-μV/cm criteria). Then, a pair of test conductors for the joint test was fabricated by slicing one stacked conductor with a diamond saw inclined at a 45° angle. The joint surfaces were then polished with #1500 abrasive grit. Fig. 3 shows the surface profile of the polished joint surface of the stacked GdBCO tapes' region, measured along the thickness direction of the tapes by a surface roughness tester. Based on the result, the arithmetic average of the surface roughness is 0.507 μm.

The experimental setup shown in Fig. 2 can apply perpendicular and parallel joint pressures to the joint section. The perpendicular pressure is generated by the rod and monitored by a load cell. The parallel one is generated by tightening the nut and the stud with a certain torque. In this experiment, the perpendicular force was varied from 3.92 to 5.88 kN and the parallel force was generated by applying a torque of 1.8 Nm at room temperature. Then, the test section was immersed in liquid nitrogen. The joint pressure on the joint surface (joint stress) at room temperature is estimated to be 185–237 MPa.

The joint resistances for four contact surface configurations (as shown in Fig. 4) were evaluated, namely, Type A (indium film), Type B (silver on one side), Type C (silver on both sides), and Type D (silver on both sides and indium film). The silver layer is made using a magnetron sputtering system. The joint resistance was evaluated with a voltage drop across the voltage taps for an applied current of 300 A.

Fig. 5 shows the joint resistance for several joint stresses for the configurations shown in Fig. 4. The points in Fig. 5 show the averaged values of two experimental measurements, and the error bar shows the maximum and the minimum values. The electrical resistances of the inserted indium film and the sputter-deposited silver layer are estimated to be 0.04 $\mu\Omega$ and 0.13 nΩ, respectively, which are lower than 5% of the measured joint resistance. Therefore, the indium film and the silver layer resistances are negligible in evaluating the joint resistance.

The results show that the contact resistance of the non-sputter-deposited surface is large since the joint resistance of Type B is about 1.6 times larger than that of Type C. In terms

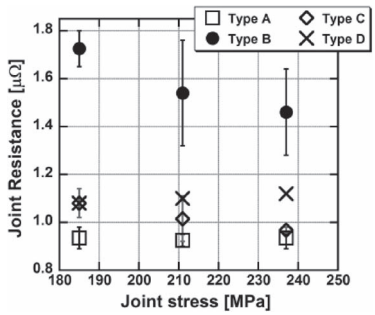

Fig. 5. Experimentally evaluated joint resistance depending on joint stress in the butt joint at 300 A.

TABLE I
STRUCTURES AND JOINT RESISTANCES FOR THE TEST CONDUCTORS

Type	Structures of the conductive metal layer of GdBCO tape	Existence of insulating tape as shown Fig. 2.	Joint resistances by joint tests
Conductor A	Silver (20 μm)	Non-existent	0.98 μΩ
Conductor B	Silver(20 μm), Solder, Copper (100 μm)	Non-existent	0.59 μΩ
Conductor C	Silver (20 μm), Solder, Copper (100 μm)	Existent	0.89 μΩ

of Type A and Type D, the joint resistance of Type D is larger than that of Type A because of the increased number of interfaces; Type A has two interfaces between the joint surface and the indium film; Type D has two interfaces between the joint surface and the silver layer and two interfaces between the silver layer and the indium film. It should be noted that the joint resistances of Type A and Type D configurations are not sensitive to the joint stress and have low spread. The indium film has thickness to accommodate a surface roughness value of about 4.5 μm. In contrast, the joint resistances of Type B and Type C, silver sputter deposited, decrease with an increase in the joint stress from 185 to 237 MPa, decreasing by 14% and 10%, respectively. The contact resistance across the two sputter-deposited silver layers is large for low joint stress because the 1-μm-thick silver layer was less than the surface roughness and does not fill interstices between the joint surfaces. Particularly in Type B, this phenomenon became prominent. Hence, the contact resistance for low joint stresses could be reduced by plating a metal layer having sufficient thickness to accommodate the surface roughness.

B. Numerical Evaluation

In this section, a 3-D numerical model is used to simulate the conductor and the joint region. In this analysis, the Type A configuration is used. This configuration shows the lowest joint resistance, as described in Section II-A. Then, the contact resistivity between the contact surface of the conductor and the indium film is evaluated by comparing experimental results with numerical results for three different conductor structures. Table I lists the different structures and the minimum measured joint resistances. Conductors A and B were used in joint tests of the previous study [8], and conductor C was presented in Section II-A. Fig. 6 shows the numerical model

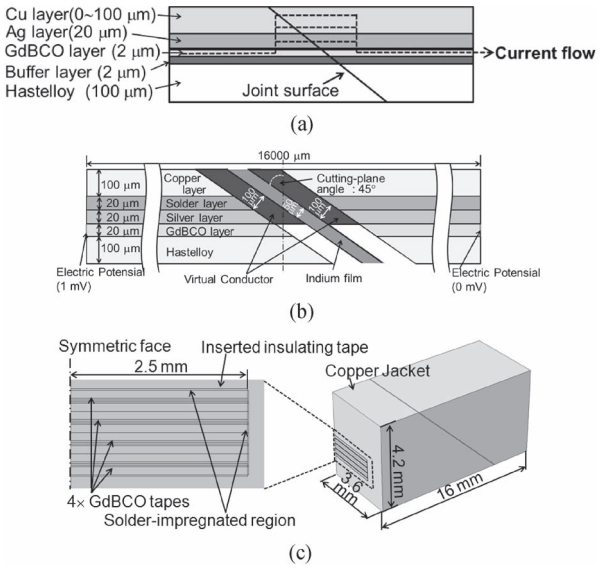

Fig. 6. Numerical model of the joint section. (a) Current pathway in the butt joint. (b) Model of the GdBCO tape. (c) Model of the stacked GdBCO conductor within a copper jacket.

for conductor C. In this analysis, we assumed uniform current distribution in the HTS region with extremely small resistivity. Contact resistance between the joint surface and the indium film was modeled by using a virtual conductor between the conductive metal (copper, solder, and silver) layers and the copper jacket, assuming that the contact resistivity of the conductive metal region RS_{Tape} is not equivalent to that of the copper jacket region RS_{Jacket} because of distributed contact pressure. Nothing was placed in the contact region of the GdBCO and Hastelloy layers to simulate that no current passes there. A 100-μm-thick solder-impregnated region was placed between stacked GdBCO tapes and the copper jacket. Furthermore, a contact resistivity of 1 Ωm^2 was set on the boundary surface between the Hastelloy and GdBCO layers to simulate the insulating buffer layer and on the top of the stacked GdBCO tapes to simulate the inserted insulating tape in conductor C. Table II shows the electrical resistivities of the constituted materials. The electrical resistivities of the solder layer and the solder-impregnated region were determined based on the previous studies [11], [12], which reported a joint resistivity of $3-11 \times 10^{-12}$ Ωm^2 for a soldered YBCO tape lap joint. The current distribution analysis was performed using COMSOL Multiphysics 4.2a AC/DC module. The joint resistance was evaluated by total joule loss and total voltage drop of the model. The model determines the current for a total voltage drop of 1 mV. About four million tetrahedral elements were used in the analysis. Contact resistivities RS_{Tape} and RS_{Jacket} were chosen as parameters in the analysis.

Fig. 7(a) shows the sensitivity of the joint resistance to RS_{Jacket} for conductor A under constant RS_{Tape}. Fig. 7(a) shows that the joint resistance remains approximately constant with changing RS_{Jacket}. The reason can be explained as follows: There are two current pathways in the area near the joint section, as shown in Fig. 8. The electrical resistance of the solder-impregnated region and the copper jacket in current pathway 1 is calculated to be about 2 $\mu\Omega$ by the numerical

TABLE II
ELECTRICAL RESISTIVITIES OF THE CONSTITUTED MATERIALS

Material	Electrical Resistivity (Ω·m)	Material	Electrical Resistivity (Ω·m)
Copper	0.2×10^{-8}	Hastelloy	14×10^{-8}
Silver	0.3×10^{-8}	Solder Layer of the tape	1.5×10^{-7}
GdBCO	1.0×10^{-13}	Solder-impregnated region	5.5×10^{-7}

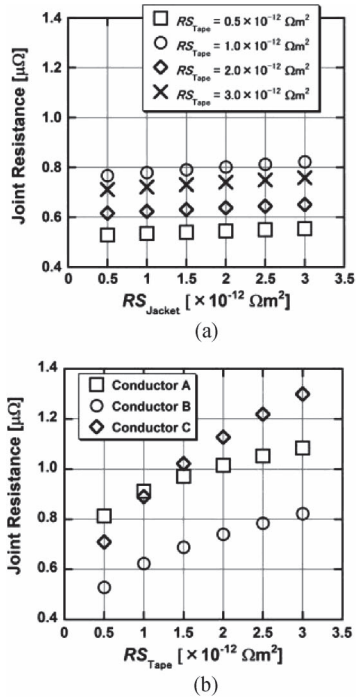

Fig. 7. Joint resistance depending on contact resistivity. (a) Copper jacket region. (b) GdBCO tape region.

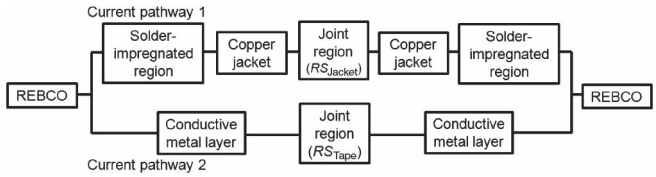

Fig. 8. Current pathway in the joint region.

results. The electrical resistance in the joint region of the copper jacket is calculated to be 0.12 $\mu\Omega$ even under the assumption that RS_{Jacket} is overestimated to be 3×10^{-12} Ωm^2, which is the joint resistivity of a soldered lap joint [11]. This value is about 6% of the former resistance, and therefore, the change in RS_{Jacket} does not affect the overall joint resistance. In the following numerical analysis, RS_{Jacket} is assumed to be zero.

Fig. 7(b) shows the relationship between the joint resistance in the conductors and RS_{Tape}. The contact resistivities for the different conductor structures are evaluated by comparing the experimental result given in Table I to the numerical result. The contact resistivities for conductors A, B, and C are estimated to be 0.9×10^{-12}, 1.0×10^{-12}, and 1.5×10^{-12} Ωm^2, respectively. The contact resistivities for the different conductor

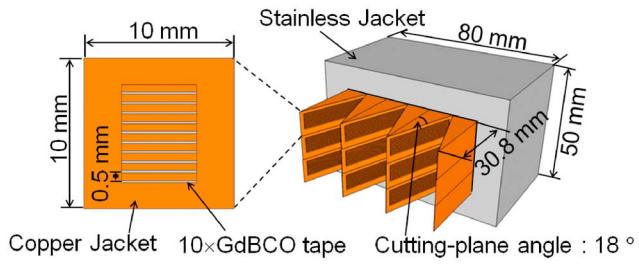

Fig. 9. Schematic views of a 100-kA-class conductor for a mechanical butt joint.

structures are similar, with an average value of 1.1×10^{-12} Ωm^2. This averaged value is almost equal to the 1.0×10^{-12} Ωm^2 contact resistivity evaluated for the mechanical butt joint where an indium film was inserted using a stacked BSCCO conductor with a copper jacket in our previous studies [4], [7].

Based on the above estimated joint resistivity, we evaluate the joint resistance of a demountable HTS magnet designed for FFHR and discuss the electric power required for cooling an entire helical coil (two helical coils). Required current for the conductor is up to 100 kA at the maximum magnetic field of up to 13 T. According to Yanagi *et al.* [12] and Terazaki *et al.* [11], the number of required 10-mm-wide REBCO tapes is about 40–100 and the operating temperature is 20 K. Fig. 9 illustrates an example for the design of a 100-kA-class REBCO conductor and the joint section for a demountable HTS magnet with mechanical butt joints, with 180 sheets of a 5-mm-wide REBCO tape. In this design, the conductor is made by a stainless jacket with 18 subconductors, each having ten REBCO tapes and a copper jacket. The thickness of the conductive metal layer of the tapes and cutting plane angle are 0.5 mm and 18°, respectively, because our latest study [8] showed that the joint resistance can be reduced by increasing the thickness and the joint angle. The joint area of the conductive metal layer of the tape in the 100-kA-class conductor is then about 36 times larger than that in the four GdBCO stacked conductors described in Section II-A. The subconductors are arranged so that the joint surface is V-shaped for compact design. Fig. 9 shows the female component of the joint. The cutting plane angle of 18° is reasonable because the length for the joint section is 30.8 mm on a half-pitch helical coil of about 12.6 m and the length for the lap joint designed by the National Institute for Fusion Science [12] of 1 m.

In this design, the joint resistance in a pair of conductors was evaluated by 3-D current distribution analysis with the numerical model of the subconductor, similar to that described earlier in this section. The joint resistance for one subconductor was estimated to be 66 nΩ, which corresponds to 660 nΩ for one REBCO tape because the subconductor consists of ten REBCO tapes. On the other hand, experimentally evaluated joint resistance for one REBCO tape was 3.56 $\mu\Omega$ based on the result for the four-layer stacked GdBCO conductor (conductor C), i.e., 0.89 $\mu\Omega$, as shown in Table I. Therefore, the joint resistance for one REBCO tape is calculated to be 18.5% of that evaluated in Section II-A. The joint resistance of the conductor consisting of 18 subconductors (each with ten tapes) is expected to be 3.7 nΩ. Using this value, the refrigeration power for the joule loss in the joint section is about 21 MW. This value is calculated under the following conditions [12]. The number of joint sections is 8000. Furthermore, based on an estimation of the cryogenic refrigeration power in the ITER design [13], we assumed that cooling power is 53 times the joule energy loss and the electric power for cooling the HTS magnet without the joint section under 20 K is about 5.7 MW. The calculated refrigeration power for the joule loss at the joint section seems to be acceptable because the required electric power for the entire FFHR refrigeration system for nuclear heating is supposed to be ~30 MW in the case of the LTS option [12].

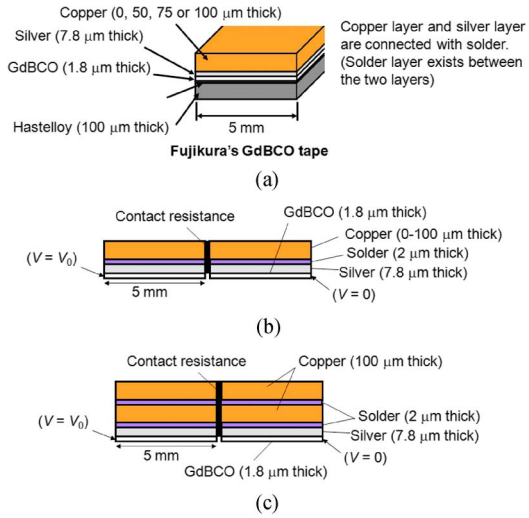

Fig. 10. Models of the edge joint of a single layer of the GdBCO tape. (a) Structure of the GdBCO tape. (b) Model of the edge joint (Type 1). (c) Model of the edge joint (Type 2).

In this evaluation, the joint resistance was evaluated based on the contact resistivity under 77 K. However, according to the theory of contact by Holm [14], the contact resistance is proportional to the resistivity of the surface material. This means that the contact resistance could decrease with a decrease in temperature. Therefore, the joint resistance and the electric power requirement should be lower when the operating temperature is 20 K.

III. Structural Improvement of the Edge Joint

A. Numerical Evaluation

In this section, we describe numerical analysis to predict joint resistance in the experiment for the edge joint of stacked REBCO conductors. We chose GdBCO tapes (FYSC-SC05, Fujikura Ltd.) having a copper stabilizer to fabricate a stacked REBCO conductor in the testing program. The GdBCO tape consists of Hastelloy substrate (100 μm)/buffer layers (0.6 μm)/GdBCO (1.8 μm)/silver (7.8 μm)/solder (2–4 μm)/copper (50, 75, or 100 μm), as shown in Fig. 10(a). In the numerical analysis, we modeled the edge joint of a single layer of the GdBCO tape. Based on the results, we designed the structure of a REBCO conductor used for the testing program of the edge joint.

Fig. 10 shows 2-D models of the edge joint of a single GdBCO tape. Fujikura Ltd. now sells several types of the GdBCO tape having different thicknesses of the copper layer (50, 75, or 100 μm). A previous study for the butt joint of a stacked REBCO conductor [8] indicated that joint resistance can be reduced by increasing the thickness of the copper layer. The joint resistance in the edge joint can be reduced also in the same manner because the current pathway in the edge joint is quite similar to that in the butt joint. We evaluated the joint resistance for two structures of HTS tape. Type 1, as shown in Fig. 10(b), models the edge joint of the single GdBCO tape where the thickness of the copper layer changes from 0 to 200 μm as a parameter; the solder region was eliminated in the case of no copper layer (0 μm). Type 2, as shown in Fig. 10(c), models the edge joint with a copper tape of 100-μm thickness soldered on the copper layer of the GdBCO tape (the thickness of the copper layer was fixed to be 100 μm). The Hastelloy and buffer layers were omitted from the models because current cannot pass to those layers. Current is assumed to be passing to the joint surface only through the conductive metal layers (silver, solder, and copper regions). Contact resistance is modeled assuming a thin zone (1-μm thick) of relatively high resistivity, in the contact region, as done in the previous section.

We used a commercial finite-element code (COMSOL Multiphysics version 4.2a) to evaluate electric potential distribution and total joule heat loss. Electric potential $V = V_0$ is applied on one outer face of the GdBCO region, and electric potential $V = 0$ (ground) is applied on the other outer face. Total joule heat loss was calculated from electric potential distribution. The joint resistance was estimated from the joule losses and V_0. The electrical conductivity values of copper and silver were determined to be 5.0×10^8 and 3.7×10^8 S/m at 77 K, respectively [15]. The resistivity of GdBCO was assumed to be 1.0×10^{16} S/m as an extremely low-resistivity material. The resistivity of the solder region was determined by experimental results for the soldered lap joint of YBCO tape [12]. The joint resistivity obtained in the study was 3.0×10^{-12} Ωm^2, and the electrical conductivity of a 2-μm soldered region is estimated to be 1.5×10^{-6} S/m.

Previous studies [7], [10] evaluated joint resistivity for mechanical joints of HTS conductors. According to [4] and [7], the joint resistivity was about 1×10^{-12} Ωm^2 for an electrical butt joint of a stacked BSCCO conductor. Another study [10] showed a joint resistivity of 4×10^{-12} Ωm^2 for an electrical lap joint. If a compliant metal layer is inserted between the joint surfaces, the joint resistivity increases because the number of interfaces doubles relative to the direct joint and the joint resistance includes resistance of the compliant metal layer itself. From the above consideration, the electrical conductivity of the contact region changed from 1.0×10^6 to 1.0×10^5 S/m as a parameter, which corresponds to a contact resistivity change from 1.0×10^{-12} to 1.0×10^{-11} Ωm^2.

Fig. 11 shows the calculated joint resistance times unit joint length as a function of the thickness of the copper layer for three cases of the contact resistivities. Those in Type 2 are indicated at the thickness of 200 μm. This result shows that the joint resistance decreases with increasing thickness of the copper layer. The joint resistance is not sensitive to the presence of the soldered region between the copper layer and the copper tape. Therefore, the joint resistance can be reduced by stacking REBCO tapes with copper tapes.

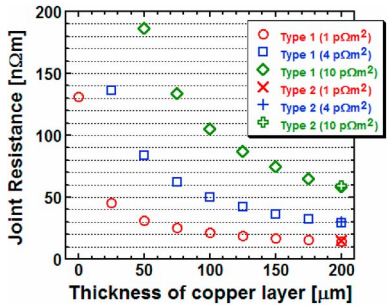

Fig. 11. Joint resistance times unit joint length in the edge joint of a single layer of the GdBCO tape depending on the thickness of the copper layer.

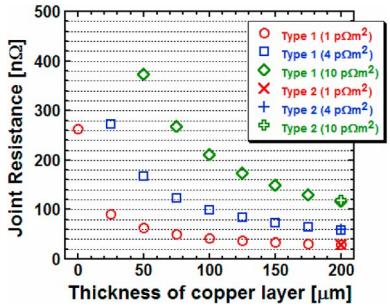

Fig. 12. Joint resistance in the edge joint of ten-layer stacked GdBCO conductors with 50-mm joint length depending on the thickness of the copper layer.

We fabricated ten-layer stacked GdBCO conductors for the testing program of the edge joint, whose critical currents were predicted to be from 1 to 2 kA, limited by our DC current supply. Furthermore, we chose two conductor structures; one is Type 1 with a 100-μm-thick copper layer, and the other is Type 2. Fig. 12 shows the joint resistance in the case of the ten-layer stacked GdBCO conductors and for a joint length of 50 mm, which would be actually used in the testing program of the edge joint. From the numerical evaluation in a previous study [4], joint resistance in a direct joint (dry joint) is strongly influenced by misalignment of the joint region, whereas when an indium film compliant layer is inserted, the joint resistance is relatively constant even if misalignment occurs. Therefore, in the testing program, we used a 100-μm-thick indium film inserted in the joint region. Joint resistivity corresponding to the indium film is about 1.5×10^{-12} Ωm^2. The joint resistivity due to the indium film compliant layer is predicted to be from 3.5×10^{-12} to 9.5×10^{-12} Ωm^2 based on joint resistivities obtained in a direct joint by previous studies [7], [10] and the existence of two interfaces. From the numerical prediction in this paper, the joint resistance should be less than 200 nΩ.

B. Experimental Evaluation

In this section, we describe the fabrication process and the joint test of stacked GdBCO conductors within a copper jacket for a testing program of the edge joint.

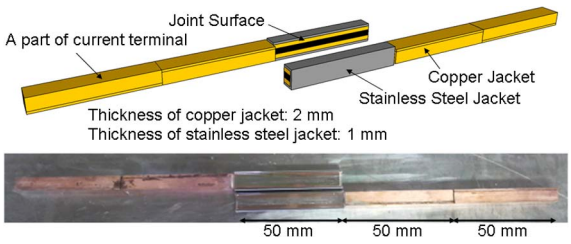

Fig. 13. Test conductors for the edge joint.

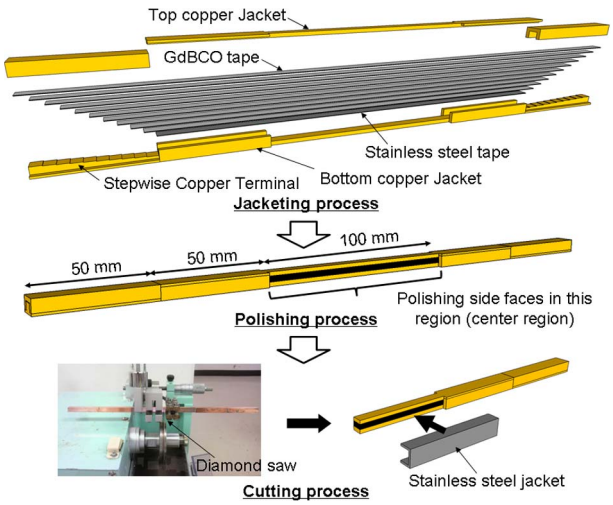

Fig. 14. Fabrication processes of the test conductors.

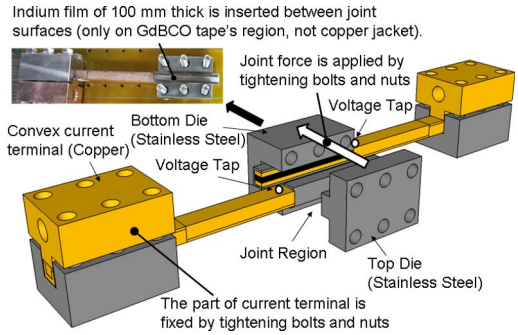

Fig. 15. Experimental setup for the electrical edge joint.

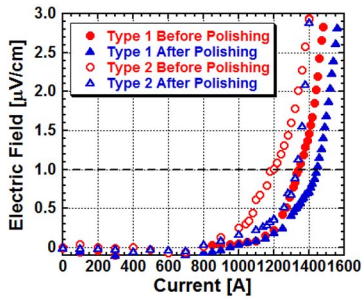

Fig. 16. Current–electric field characteristics of the test conductors before and after the polishing process.

As mentioned in Section III-A, we used a GdBCO tape (FYSC-SC05, Fujikura Ltd.) for the test conductors. The total thickness of the tape is 225 μm, and the width of the tape is 5 mm. The critical current of the tape is 260 A at 77 K, self-field. Fig. 13 shows the test conductors used in this paper. We prepared two types of test conductor based on the numerical analysis, i.e., Type 1 and Type 2. The two test conductors have ten GdBCO tapes in copper jackets. The specification of the tape is the same as described in the previous section. Type 2 conductors also have ten copper tapes, 100-μm thick. Current is applied through a stepwise current terminal to each GdBCO tape.

Fig. 14 shows the procedure to fabricate the test conductors. The first step was the jacketing process. Ten GdBCO tapes coated with Sn63Pb37 solder were stacked inside the bottom copper jacket on a hot plate whose temperature was set to 210 °C. In the cases of Type 2 conductor, copper tapes also coated with the solder were stacked on the copper surface of each GdBCO tape. A stainless steel tape coated with the solder was also inserted between the copper jacket and the copper layer or the copper tape to minimize current from the GdBCO tape flowing through the copper jacket. Finally, the bottom copper jacket was closed with a copper top plate. In the jacketing process, we used soldering flux for stainless steel to coat the Hastelloy surface and stainless steel tape with the solder. The stepwise current terminals were soldered to each GdBCO tape's copper layer surface.

After fixing the current terminals, the critical current of the center part was evaluated in liquid nitrogen. This region, after polishing, is used as the joint surface for the electrical edge joint. The second step was the polishing process. In the previous study [4], YBCO tapes used for the test conductor were degraded by a milling process. The shape of the jacket in this paper eliminates the need for milling. Only the side faces of the central region were polished with #600 abrasive. At the same time, parallelism tolerance for both side faces was controlled to be less than 0.01 mm, which is less than one tenth of the thickness of the inserted indium film.

After polishing, the critical current was measured in liquid nitrogen again to determine conductor degradation due to polishing. Finally, the polished test conductors were cut by a diamond saw. The stainless steel jacket was fixed to the joint section to prevent deformation by the joint force.

Fig. 15 illustrates the experimental setup. Copper current terminals of convex shape were mechanically fixed to the part of the stepwise current terminal of the test conductor by tightening bolts and nuts. An indium film of 100-μm thickness was also inserted between the convex-shaped copper terminal and the part of the stepwise terminal. The torque on the bolts on the terminal section was adjusted for a joint stress of 100 MPa. The edge joint part was fixed with stainless steel top and bottom dies. An indium film of 100-μm thickness was inserted between joint surfaces (only on GdBCO tape's region, not copper jacket). Joint force was adjusted by tightening the bolts. The joint stress was calculated by torque (axial force of the bolts) and joint area. Joint resistance was estimated by applied current and voltage drop between the voltage taps in liquid nitrogen.

Fig. 16 shows the $I-E$ curves for Type 1 and Type 2 conductors before and after polishing the center part. Critical currents of Type 1 and Type 2 decreased from 1340 to 1200 A and from 1450 to 1320 A, respectively (1-μV/cm criteria). The

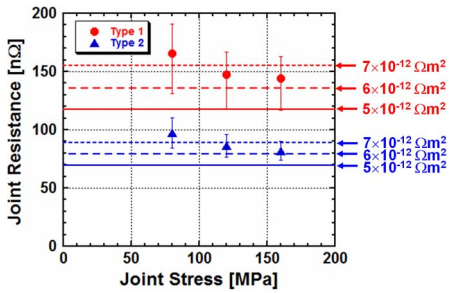

Fig. 17. Joint resistance as a function of joint stress obtained by the testing program of the edge joint at 1000 A.

polishing process degraded the critical current by about 10% due to a change in the width of the GdBCO tape (changed from 5 to 4.5 mm by the polishing process). Therefore, critical current density was not degraded by polishing process.

Fig. 17 shows joint resistance as a function of joint stress. Plotted symbols indicate an averaged value of several experiments, and error bars indicate the maximum and the minimum values. Three lines show the numerical predictions when the contact resistivity is set to 5, 6, and 7×10^{-12} Ωm^2. The evaluated joint resistivity was similar to those evaluated in some previous studies [7], [10] and Section II of this paper. Therefore, good edge joint performance was demonstrated by an improved fabrication process, as compared to a previous study [4].

We can also use the results to predict joint resistance for large-scale HTS conductors having the edge joint. As mentioned in Section II, 80–200 REBCO tapes of 5-mm thickness are needed to achieve a 100-kA-class HTS conductor at 20 K. The joint resistance of an edge joint with a joint length of 500 mm and the structure of the Type 2 conductor can be estimated to be 0.4–1.0 nΩ. The value is sufficiently small to apply the edge joint to a demountable HTS magnet from a viewpoint of electric power for cooling according to the discussion in Section II. In addition, we also expect that the value can be reduced at lower temperature based on the contact theory, as also mentioned in Section II.

IV. Conclusion

In this paper, we have summarized recent research on demountable butt and edge joints in series. Based on small-scale experiments and current distribution analyses of the butt joint, we have established a method for predicting joint resistance of a large-scale conductor. We have also tested electrical edge joints with an improved fabrication process and structure. The experimentally obtained joint resistance agreed with the numerical prediction. Good edge joint performance was demonstrated by using the improved test conductors. We have predicted the joint resistance for large-scale HTS conductors and shown that it is sufficiently small so that the demountable HTS magnet can be practical, with low dissipation and electrical cooling power.

References

[1] L. Bromberg, M. Tekula, L. A. El-Guebaly, and R. Miller, "Options for the use of high temperature superconductor in tokamak fusion reactor designs," *Fus. Eng. Des.*, vol. 54, no. 2, pp. 167–180, Feb. 2001.

[2] L. Bromberg, H. Hashizume, S. Ito, J. V. Minervini, and N. Yanagi, "Status of high temperature superconducting fusion magnet development," *Fusion Sci. Technol.*, vol. 60, no. 2, pp. 635–642, Aug. 2011.

[3] Z. S. Hartwig, C. B. Haakonsen, R. T. Mumgaard, and L. Bromberg, "An initial study of demountable high-temperature superconducting toroidal field magnets for the Vulcan tokamak conceptual design," *Fusion Eng. Des.*, vol. 87, no. 3, pp. 201–214, Mar. 2012.

[4] S. Ito, L. Bromberg, M. Takayasu, J. V. Minervini, and H. Hashizume, "Proposal of electrical edge joint for a demountable high-temperature superconducting magnet," *IEEE Trans. Plasma Sci.*, vol. 40, no. 5, pp. 1446–1452, May 2012.

[5] H. Hashizume, S. Kitajima, S. Ito, K. Yagi, Y. Usui, Y. Hida, and A. Sagara, "Advanced fusion reactor design using remountable HTc SC magnet," *J. Plasma Fusion Res. Ser.*, vol. 5, pp. 532–536, 2002.

[6] S. Ito and H. Hashizume, "Overview of fundamental study on remountable HTS magnet," *Fusion Eng. Des.*, vol. 81, no. 20–22, pp. 2527–2533, Nov. 2006.

[7] S. Ito and H. Hashizume, "Investigation of an optimum structure for mechanical butt joint of a stacked HTS cable with a metal jacket," *IEEE Trans. Appl Supercond.*, vol. 21, no. 3, pp. 1995–1999, Jun. 2011.

[8] T. Ohinata, S. Ito, and H. Hashizume, "Fundamental evaluation of joint resistance in mechanical butt joint of a stacked GdBCO conductor," *Plasma Fus. Res.*, vol. 7, p. 2405045, May 2012.

[9] A. J. Dietz, W. E. Audette, L. Bromberg, J. V. Minervini, and B. K. Fitzpatrick, "Resistance of demountable mechanical lap joints for a high temperature superconducting cable connector," *IEEE Trans. Appl. Supercond.*, vol. 18, no. 2, pp. 1171–1174, Jun. 2008.

[10] S. Ito and H. Hashizume, "Transverse stress effects on critical current and joint resistance in mechanical lap joint of a stacked HTS conductor," *IEEE Trans. Appl. Supercond.*, vol. 22, no. 3, p. 6400104, Jun. 2012.

[11] Y. Terazaki, N. Yanagi, S. Tomida, H. Noguchi, K. Natsume, T. Mito, S. Ito, H. Hashizume, and A. Sagara, "Measurement of the joint resistance of large-current YBCO conductors," *Plasma Fus. Res.*, vol. 7, p. 2405027, May 2012.

[12] N. Yanagi, T. Mito, R. Champailler, G. Bansal, H. Tamura, and A. Sagara, "Design progress on the high-temperature superconducting coil option for the heliotron-type fusion energy reactor FFHR," *Fusion Sci. Technol.*, vol. 60, no. 2, pp. 648–652, Aug. 2011.

[13] J. L. Duchateau, J. Y. Journeaux, and F. Millet, "Estimation of the recycled power associated with the cryogenic refrigeration power of a fusion reactor based on TORE SUPRA experiment and ITER design," *Nucl. Fusion*, vol. 46, no. 3, pp. S94–S99, Mar. 2006.

[14] R. Holm, *Electric Contacts Theory and Application*. Boulder, CO, USA: Springer-Verlag, 1967.

[15] J. W. Ekin, *Experimental Techniques for Low-Temperature Measurements: Cryostat Design, Material Properties, and Superconductor Critical-Current Testing*. Boulder, CO, USA: Oxford Univ. Press, 2006.